J Nanostruct 16(4): 5121-5130, Autumn 2026

RESEARCH PAPER

Highly Efficacious Synthesis of Spiro-Fused Oxindole-Dioxolo[g][1]benzopyran Derivatives by Mechano-Chemical Approach using Ti_3C_2OH MXene 2D Nanomaterial

Farshad Ghanbili [1], ***Shahrzad Abdolmohammadi*** [2*], ***Simin Janitabardarzi*** [3]

[1] *Department of Mechanical Engineering, K.N. Toosi University of Technology, Tehran, Iran*

[2] *Department of Chemistry, ST.C., Islamic Azad University, Tehran, Iran*

[3] *Nuclear Science and Technology Research Institute, P.O. Box 11365-8486, Tehran, Iran*

ARTICLE INFO

Article History:
Received 10 June 2026
Accepted 05 August 2026
Published 01 October 2026

Keywords:
Ethanol-assisted grinding
Green approach
Spiro-fused oxindole-dioxolo[g][1]benzopyrans
Ti_3C_2OH MXene

ABSTRACT

Mechano-chemistry has recently been used to carry out some of the processes for more sustainable chemical synthesis. This technique is seen to be appealing and environmentally friendly since it allows for solvent-free reactions or the use of activators for the reaction, which makes the process affordable and efficient. In the current work, the Ti_3AlC_2 MAX phase was synthesized using a mechanochemical grinding ball mill method, and then it was converted into Ti_3C_2OH MXene, a new, eco-friendly, effective, and recyclable nanocatalyst. Spectroscopic and microscopic methods (FT-IR, XRD, SEM, and EDS) were used to characterize prepared MAX and Mxene. The prepared Ti_3C_2OH MXene was utilized for the synthesis of spiro-fused oxindole-dioxolo[g][1]benzopyran derivatives by a mechanochemical grinding approach. This technique produced a number of target compounds with high yields and quick reaction times by reacting 3,4-methylenedioxyphenol, malononitrile, and 5-substituted isatins. Moreover, MXene was easily removed from the reaction mixture and used five more times without substantially changing its catalytic activity.

How to cite this article
Ghanbili F, Abdolmohammadi SH, Janitabardarzi S. Highly Efficacious Synthesis of Spiro-Fused Oxindole-Dioxolo[g][1]benzopyran Derivatives by Mechano-Chemical Approach using Ti_3C_2OH MXene 2D Nanomaterial. J Nanostruct, 2026; 16(4):5121-5130. DOI: 10.22052/JNS.2026.04.052

INTRODUCTION

The use of multi-component reactions (MCRs) as adaptable reactions to produce a wide variety of complex compounds with frequently biologically relevant scaffold structures using novel, efficient methods has become recognized as an intriguing and eco-friendly strategy [1]. According to published research, the mechano-chemistry method has created a chance to create novel processes for the quick synthesis of organic compounds since it allows for solvent-free reactions or the use of activators, which makes the process effective and affordable [2].

Among the various number of natural and unnatural bio-active spirocycles discovered heretofore, the spirooxindole moiety is a clinically significant drug used in the treatment and management of many diseases [3, 4]. Strong biological activities, such as antioxidant [5], antibacterial [6], antiviral [7], anticancer [8, 9], and antimalarial effects [10], are displayed by compounds with the spirooxindole structure. The

* *Corresponding Author Email: s.abdolmohamadi@yahoo.com*

importance of the spirooxindole framework in drug development is shown by the fact that it is present in many naturally occurring medicinally useful compounds. Typical examples with anti-inflammatory, anti-malarial, antimicrobial, and antitumor properties include mitraphiline [11], KAE609 [12], elacomine [13], and spirotryprostatin A [14] (Fig. 1).

The MAX phases encompass a diverse category of stratified materials, consisting of hexagonal ternary early transition metal nitrides, carbides, and carbonitrides. This material demonstrated advantageous factors such as excellent thermal and electrical conductivity, ease of machinability, and resistance to oxidation and thermal shocks. They coined the term "$M_{n+1}AX_n$" phase (where n = 1, 2, or 3), or "MAX" phase, to refer to these materials. In this material, M is a transition element, A is an element from the A group (group IIIA or IVA), and "X" represents carbon and/or nitrogen [15]. The MAX phases demonstrate chemical stability, although the A layers exhibit higher chemical reactivity due to the relatively weak M-A bonds between the $M_{n+1}X_n$ layers. Hence, the Ti element can be reacted with Al and C to produce Ti_3AlC_2 or Ti_2AlC MAX phases. Next, during the etching and

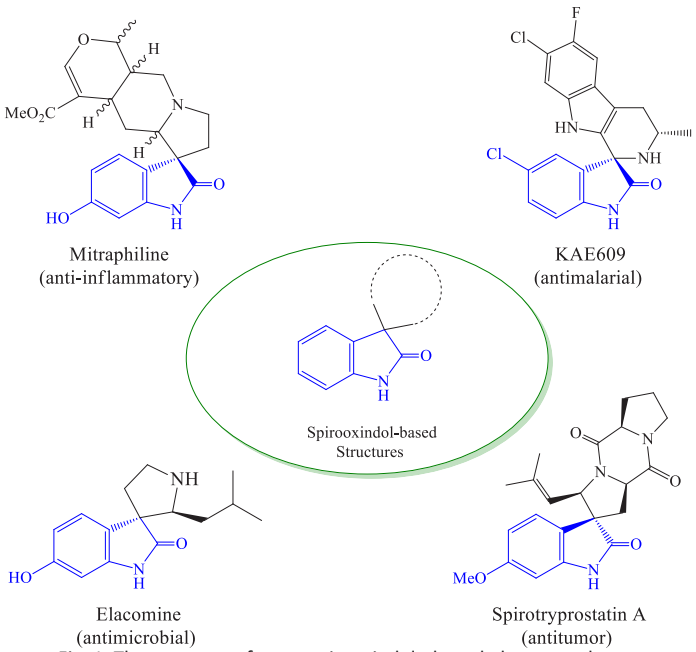

Fig. 1. The structure of some spirooxindole-based pharmacophores.

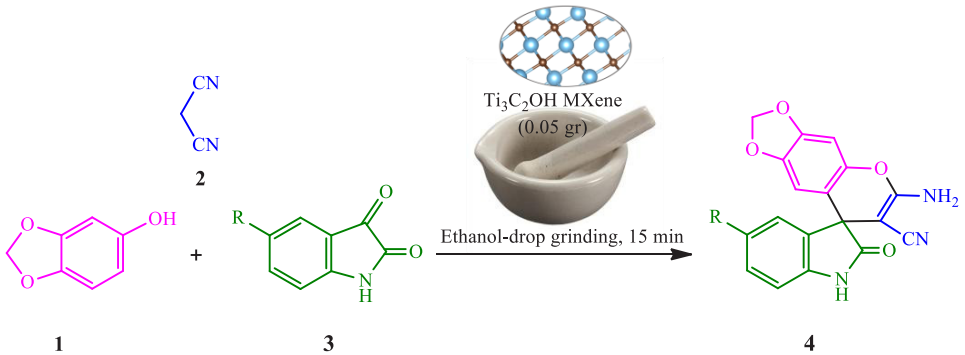

Fig. 2. Cyclocondensation reaction of 3,4-methylenedioxyphenol, malononitrile, and 5-substituted isatins using Ti_3C_2OH MXene under grinding.

delaminating procedures, the alumina is removed through centrifugation. The resulting colloidal suspension includes new materials denoted as MXene [16].

According to a review of the literature, one of the most important and desirable methods for chemists to promote environmentally friendly and sustainable chemical processes is the use of nanostructured materials as potential heterogeneous catalysts [17]. Since its discovery in 2011, MXenes, a form of two-dimensional material, have attracted a lot of attention due to their efficacy in certain situations [18]. These layered materials on a two-dimensional plane have sheet topologies similar to graphene, as indicated by the suffix "ene" in MXenes [18]. The usual formula for MXene is $M_{n+1}X_nT_x$, where n can be any number between 1 and 3. T stands for surface terminal functions, such as OH, O, F, and Cl, and M can be a transition metal atom, such as Zr, V, Ti, or Sc, positioned between n layers of either nitrogen or carbon (referred to as X) [19].

Here, we report for the first time on the catalytic use of Ti_3C_2OH MXene in the synthesis of a series of spiro-fused oxindole-dioxolo[*g*][1]benzopyran derivatives (4), considering our expertise in designing and developing new catalyzed synthetic methods for the preparation of significant heterocyclic frameworks [20-23]. The title compounds were produced by employing Ti_3C_2OH MXene as a novel, superior catalyst in a three-component reaction involving 3,4-methylenedioxyphenol (1), malononitrile (2), and 5-substituted isatins (3) utilizing a mechanochemical ethanol-assisted grinding technique (Fig. 2). Despite our previous publication on a practical approach, this work provides a recoverable catalyst/grinding-aid system and is strongly compatible with the concepts of green chemistry [24].

MATERIALS AND METHODS

Chemical reagents and solvents were purchased from Merck and Fluka Companies and utilized without additional purification. IR spectra were recorded on an ABB FT-IR (FTLA 2000) spectrometer. ^1H NMR and ^{13}C NMR spectra were recorded on a Bruker DRX-500 AVANCE at 500 and 125 MHz, respectively, in DMSO-d_6 as the solvent and TMS as the internal standard. Elemental analyses were performed on a Foss-Heraeus *CHN*-O-rapid analyzer. X-ray diffraction (XRD) was recorded on a Philips PW1800/00 X-ray powder diffractometer employing CuKα X-ray radiation (0.154056 nm). Scanning electron microscopy (SEM) was captured with a TESCAN Vega TS 5136LM coupled to an energy-dispersive X-ray (EDS) detection system, typically at an acceleration voltage of 20 Kv.

General procedure for the synthesis of Ti_3AlC_2 MAX phase

The milling process was performed in order to synthesize Ti_3AlC_2 MAX phase in Ti–Al–C system. For this purpose, a mixture of commercially available powders of Ti, Al, and C with a stoichiometric ratio corresponding to the preparation of Ti_3AlC_2, with Ti:Al:C = 3:1:2, was milled by a planetary ball mill for 10 h. A milling chamber made of tungsten carbide of 220 mL volume and balls made of zirconia of 2-8 mm diameter were applied for the milling operation.

General procedure for the synthesis of Ti_3C_2OH MXene Nanomaterial

The Ti_3C_2OH MXene was prepared using selective etching of Al from the prepared Ti_3AlC_2 MAX phase in the HF solution [25]. In a typical synthesis process, 2 g of the prepared MAX powders were slowly added to 50 mL of HF solution (40 wt%). The etching process was continued for 24 h, while stirring proceeded with the help of a magnetic Teflon-coated bar. Next, the mixture was washed several times with deionized water and finally centrifuged. After that, the powder samples were washed with ethanol and dried in a vacuum oven.

General procedure for the preparation of compounds 4a-g

A mixture of 3,4-methylenedioxyphenol (1, 1 mmol), malononitrile (2, 1 mmol), 5-substituted isatins 3 (1 mmol), and Ti_3C_2OH MXene (0.05 g) was grinded with a mortar and pestle at room temperature, in the presence of small amounts of ethanol, for about 20 minutes. TLC in a 3:2 ethyl acetate/n-hexane TLC solvent was used to monitor the reaction's progression. After the reaction was finished, the reaction mixture was dissolved in 3 mL of hot ethanol and centrifuged for five minutes at 2000-3000 rpm to extract the catalyst for reuse. The mixture was then repeatedly rinsed with ethanol and dried. The ethanol solution was cooled to room temperature, diluted with 1 mL of water, and then allowed to crystallize to produce the pure product.

Spiro[3,8′]5-bromo-1,3-dihydro-2H-indol-2-one-6′-amino-8′H-[1′,3′]dioxolo[4′,5′-g][1]benzopyran-7′-yl cyanide (4b)

White powder, m.p. 355-357 ˚C, yield: 0.387 g (94%). IR (KBr): ν_{max} 3324, 3289, 3228, 2862, 2119, 1660, 1541, 1325, 1218 cm^{-1}. ^1H NMR (500 MHz, DMSO-d_6): δ 5.86 (1 H, d, J = 1.2 Hz, CH_2), 5.96 (1 H, d, J = 1.2 Hz, CH_2), 7.33 (1 H, brd, J = 7.9 Hz, HAr), 7.47 (1 H, s, HAr), 7.58 (1 H, s, HAr), 7.62 (2 H, brs, NH_2), 7.81 (1 H, m, HAr), 7.90 (1 H, s, HAr), 10.93 (1 H, s, NH) ppm. ^{13}C NMR (125 MHz, DMSO-d_6): δ 59.6, 73.6, 97.6, 102.2, 104.5, 107.9, 116.1, 117.9, 123.0, 124.2, 128.4, 130.9, 144.9, 147.7, 146.4, 148.2, 159.4, 172.7 ppm. Anal. Calcd for $C_{18}H_{10}BrN_3O_4$ (412.19): C 52.45, H 2.45, N 10.19; Found: C 52.31, H 2.62, N 10.30.

Spiro[3,8′]1,3-dihydro-5-hydroxy-2H-indol-2-one-6′-amino-8′H-[1′,3′]dioxolo[4′,5′-g][1]benzopyran-7′-yl cyanide (4d)

Pale yellow powder, m.p. 319-321 ˚C, yield: 0.325 g (93%). IR (KBr): ν_{max} 3368, 3276, 3213, 2944, 2112, 1664, 1533, 1334, 1210 cm^{-1}. ^1H NMR (500 MHz, DMSO-d_6): δ 5.79 (1 H, d, J = 1.2 Hz, CH_2), 5.86 (1 H, d, J = 1.2 Hz, CH_2), 6.88 (1 H, brd, J = 7.5 Hz, HAr), 7.04 (1 H, s, HAr), 7.53 (1 H, s, HAr), 7.67 (2 H, brs, NH_2), 7.75 (1 H, brd, J = 7.5 Hz, HAr), 7.89 (1 H, s, HAr), 9.31 (1 H, s, OH), 11.02 (1 H, s, NH) ppm. ^{13}C NMR (125 MHz, DMSO-d_6): δ 60.0, 74.5, 99.3, 101.8, 103.8, 108.6, 114.3, 118.4, 122.7, 125.3, 129.6, 144.6, 146.1, 147.4, 148.5, 158.6, 160.1, 173.4 ppm. Anal. Calcd for $C_{18}H_{11}N_3O_5$ (349.30): C 61.89, H 3.17, N 12.03; Found: C 62.07, H 3.27, N 11.91.

RESULTS AND DISCUSSION

The main aim of this research, as shown in Fig. 2, is to develop the catalytic applications of the Ti_3C_2OH MXene 2D nanomaterial for the environmentally friendly synthesis of a series of spiro-fused oxindole-dioxolo[g][1]benzopyrans. Ti_3C_2OH MXene was obtained through HF etching of Ti_3AlC_2 MAX phase, while the MAX phase precursor was synthesized using a ball milling-assisted method that reduces energy consumption and improves the sustainability of the overall preparation process [25]. The EDS analysis confirms the presence of oxygen on the $Ti_3C_2T_X$ surface, signifying the successful formation of oxygen-containing functional groups as a hallmark of etched MXene materials. The structural correctness of the synthesized nanomaterial was then assessed using several techniques, including X-ray diffraction (XRD) analysis, scanning electron microscopy (SEM), and energy dispersive X-ray spectrometry (EDS). The XRD patterns of the separated pure objects, Ti_3AlC_2 MAX and Ti_3C_2OH nanomaterials, are illustrated in Fig. 3.

According to the XRD analysis, the peaks corresponding to Ti_3AlC_2 MAX and Ti_3C_2OH were observed, while Ti_3AlC_2 was the main phase. By transforming the Ti_3AlC_2 MAX phase into Ti_3C_2OH MXene, a remarkable shift of the (002) plane to the lower angles and vanishing of the sharpest peak of Ti_3AlC_2 at 2θ = 39˚ in the XRD patterns can be observed. These changes reveal the successful conversion of Ti_3AlC_2 into Ti_3C_2OH [26]. The (002) diffraction peak at an angle of 6.6˚ can be utilized for the assessment of the d-spacing between the

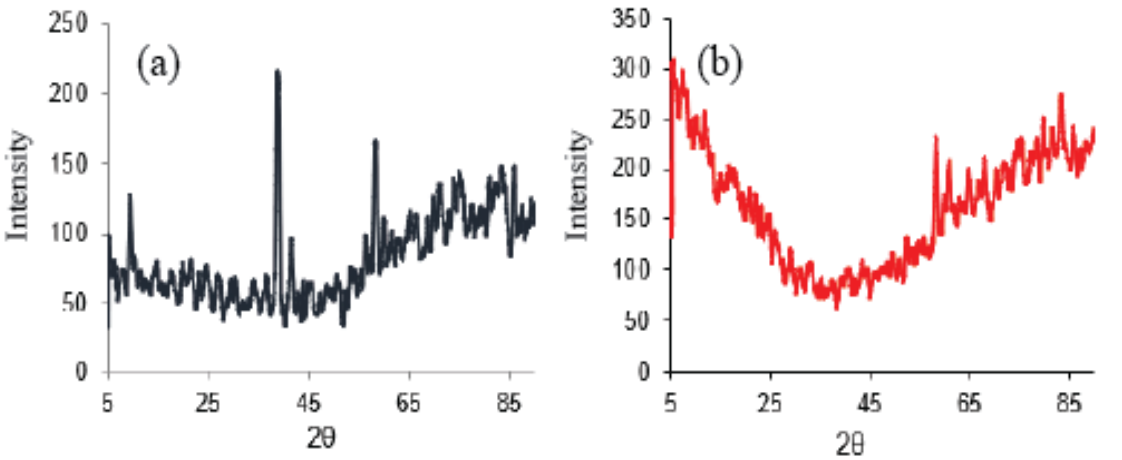

Fig. 3. XRD patterns of the synthesized Ti_3AlC_2 MAX (a), and Ti_3C_2OH MXene (b).

MXene nanosheets and the monolayer thickness. Compared to the MAX phase precursor, the etching procedure yielded MXene with expanded interlayer spacing, evidenced by an increase in the c-lattice parameter of their crystallites.

Fig. 4 shows the SEM micrograph of the MAX product after 10 h milling and its EDX analysis. The layer structure of Ti_3AlC_2 together with granular grains can be seen. The formation of the observed agglomerates suggested that a mechanically induced self-propagating reaction occurred. This procedure releases a large amount of heat, which not only makes reactions occur but also raises the temperature in the microzone at a high level, resulting in the sintering of small parts of powders to coarse granules. However, this agglomerate can easily be de-agglomerated [27]. The existence of Ti, Al, and C elements and their elemental percentage can be confirmed via the EDX curve and the presented elemental maps.

According to Fig. 4g, a more developed layered structure of MXene can be observed, indicating the efficient removal of Al from the MAX phase. The EDS analysis shows that Al was drastically

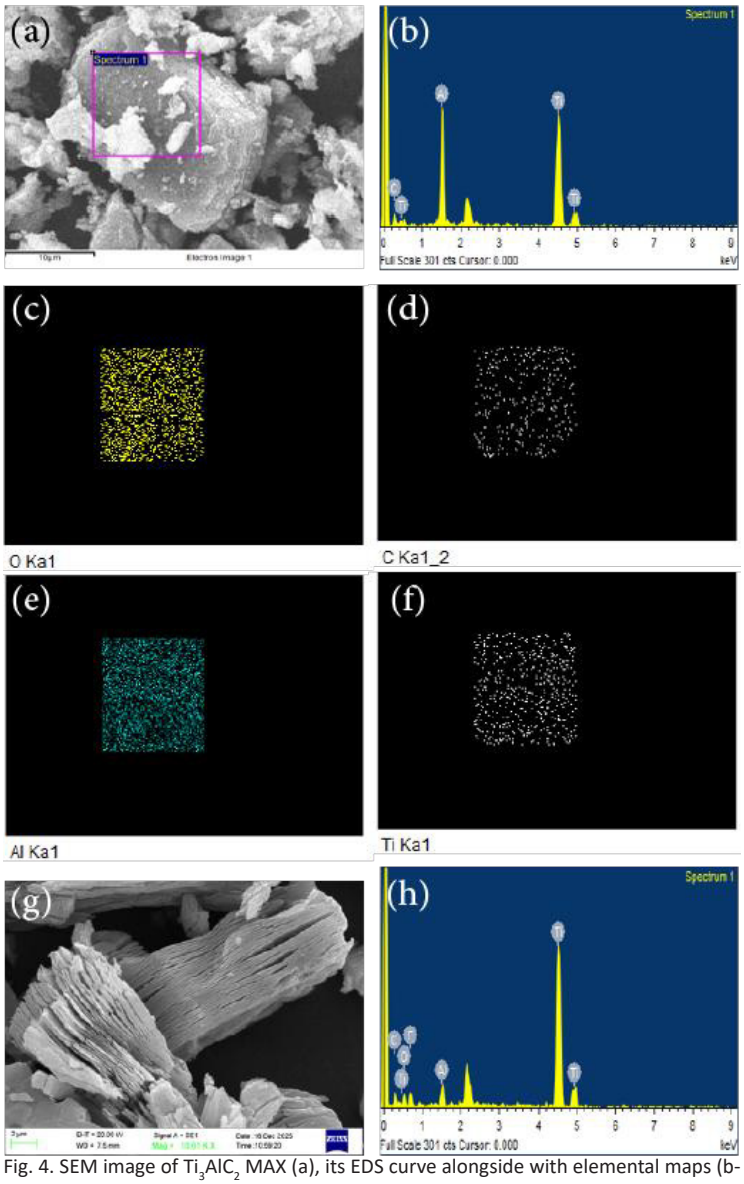

Fig. 4. SEM image of Ti_3AlC_2 MAX (a), its EDS curve alongside with elemental maps (b-f), and SEM image of synthesized Ti_3C_2OH MXene and its EDS curve (g-h).

reduced during the etching process, confirming the near-complete extraction of Al from the parent MAX structure. The EDS spectrum confirms the presence of oxygen on the MXene surface, suggesting the existence of oxygen-containing surface terminations.

To further elucidate the chemical nature and origin of these oxygen species, FT-IR spectroscopy was employed (Fig. 5). The spectrum exhibits characteristic absorption bands at approximately 3400 and 1083 cm^{-1}, which are attributed to OH and C-O stretching vibrations, respectively. These features suggest the integration of hydroxyl and epoxy terminal groups within the MXene structure. Furthermore, the prominent peak at 563 cm^{-1} is assigned to the Ti–O lattice vibrations [28]. The sharp band at 1637 cm^{-1} corresponds to the H–O–H bending mode of structural water molecules intercalated within the MXene interlayer galleries. Notably, the absence of distinct peaks in the regions of 1700-1725 and 1210-1320 cm^{-1} confirms the lack of carboxylic groups (COOH), indicating that the surface remains free from significant oxidative degradation into organic acid forms.

As shown in Fig. 6, a typical reaction of 3,4-methylenedioxyphenol (1), malononitrile (2), and 5-bromoisatin (3b) was employed for the synthesis of compound 4b under various reaction conditions, with the results presented in Table 1. Conducting the reaction without any catalyst at reflux temperature in ethanol was examined first. After 6 hours, only 52% of the product was obtained (Table 1, entry 1). The reaction was also performed without any catalyst under ethanol-drop grinding at room temperature; a low conversion was observed on TLC after 60 minutes (Table 1, entry 2). However, this typically requires a catalyst to drive the reaction. Then, the reaction was evaluated using Ti_3C_2OH MXene as a new heterogeneous catalyst in both conditions: ethanol reflux or ethanol-drop grinding. As can

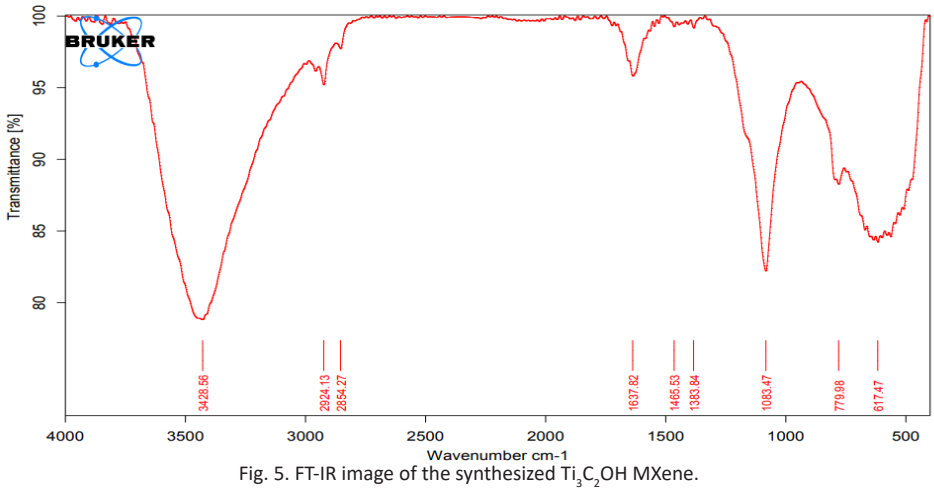

Fig. 5. FT-IR image of the synthesized Ti_3C_2OH MXene.

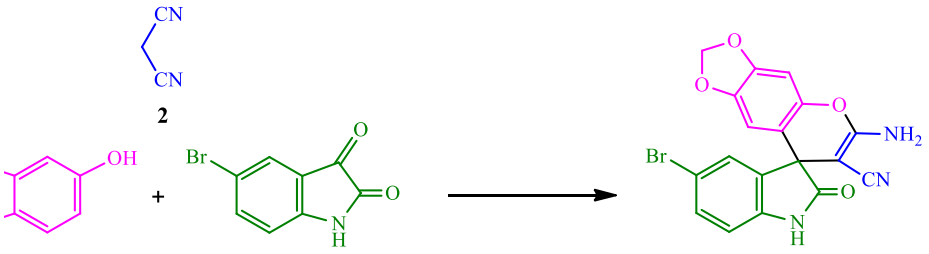

1 **3b** **4b**

Fig. 6. Synthesis of spiro[3,8′]5-bromo-1,3-dihydro-2*H*-indol-2-one-6′-amino-8′*H*-[1′,3′]dioxolo[4′,5′-*g*][1] benzopyran-7′-yl cyanide (4b) under various conditions.

be observed, grinding is more efficient than reflux and requires less reaction time and temperature (Table 1, entries 3 & 4). To identify the optimum amounts of the catalyst, the reaction was carried out with 0.04, 0.05, and 0.06 g of Ti_3C_2OH MXene; conversion yields of 80%, 94%, and 92% were obtained, respectively, after 20 minutes grinding (Table 1, entries 4-6). Next, the replacement of the Ti_3C_2OH MXene with some Brønsted acids such as HCl and *p*-TSA (*p*-toluenesulfonic acid) in the model reaction led to moderate conversions after 20 minutes grinding (Table 1, entries 4 & 6-7). Additionally, the impact of grinding duration was examined, and it was found that only 20 minutes of grinding could successfully convert the particular reactants (Table 1, entries 4 & 9-10).

We investigated the substrate scope by selecting several of 5-substituted isatins after establishing the optimal conditions for the aforementioned reaction. This was tested in the reaction with 3,4-methylenedioxyphenol, malononitrile, resulting in the production of the target compounds whitin 20 minutes in high yields (Table 2).

For the synthesis of 4b under optimal reaction conditions, the next step was to examine the

Table 1. Optimization of reaction conditions for preparation of spiro[3,8']5-bromo-1,3-dihydro-2*H*-indol-2-one-6'-amino-8'*H*-[1',3'] dioxolo[4',5'-*g*][1]benzopyran-7'-yl cyanide (4b).

Entry	Conditions	Catalyst	Time (min)	Yield (%)[b]
1	EtOH (Reflux)	-----	360	52
2	EtOH-drop Grinding	-----	20	trace
3	EtOH (Reflux)	Ti_3C_2OH MXene (0.05 g)	60	92
4	EtOH-drop Grinding	Ti_3C_2OH MXene (0.05 g)	20	94
5	EtOH-drop Grinding	Ti_3C_2OH MXene (0.04 g)	20	80
6	EtOH-drop Grinding	Ti_3C_2OH MXene (0.06 g)	20	92
7	EtOH-drop Grinding	HCl (15 mol%)	20	72
8	EtOH-drop Grinding	*p*-TsOH[a] (15 mol%)	20	65
9	EtOH-drop Grinding	Ti_3C_2OH MXene (0.05 g)	10	88
10	EtOH-drop Grinding	Ti_3C_2OH MXene (0.05 g)	25	94

[a]*p*-TsOH: *p*-Toluenesulfonic acid.
[b]Isolated yield.

Table 2. Ti_3C_2OH MXene nanostructure catalyzed syntheses of Spiro[3,8']1,3-dihydro-2*H*-indol-2-one-6'-amino-8'*H*-[1',3'] dioxolo[4',5'-*g*][1]benzopyran-7'-yl cyanides 4a-g.

Product	R	Yield (%)[a,b]	M.p (˚C)	
			Obsd.	Lit.
4a	H	90	263-264	265-267 [24]
4b	Br	94	355-357	---
4c	Cl	92	324-326	>300 [24]
4d	HO	93	319-321	---
4e	CH_3O	94	263-365	260-262 [24]
4f	H_3C	92	277-278	273-275 [24]
4g	O_2N	95	362-364	>300 [24]

[a]Yields refer to those of pure isolated products characterized by IR, ^{1}H NMR and ^{13}C NMR spectral data and by elemental analyses.
[b]Reaction conditions: A mixture of 3,4-methylenedioxyphenol (1, 1 mmol), malononitrile (2, 1 mmol), 5-substituted isatins 3 (1 mmol), Ti_3C_2OH MXene (0.05 g) was kept under ethanol-assisted grinding at room temperature for about 20 minutes.

Table 3. Recycability of the catalyst in the synthesis of spiro[3,8']5-bromo-1,3-dihydro-2*H*-indol-2-one-6'-amino-8'*H*-[1',3'] dioxolo[4',5'-*g*][1]benzopyran-7'-yl cyanide (4b).

Run	Fresh	1	2	3	4	5
Isolated yield (%)[a,b]	94	94	92	91	90	88

[a]Yields refer to those of pure isolated products characterized by IR, ^{1}H NMR and ^{13}C NMR spectral data and by elemental analyses.
[b]Reaction conditions: A mixture of 3,4-methylenedioxyphenol (1, 1 mmol), malononitrile (2, 1 mmol), 5-bromo isatin (3b, 1 mmol), Ti_3C_2OH MXene (0.05 g) was kept under ethanol-assisted grinding at room temperature for about 20 minutes.

catalyst's recyclability. The recovered catalyst can be recycled five times, although there is a slight decrease in activity (Table 3).

Fig. 7 illustrates a feasible pathway for producing product 4, based on the explanatory processes reported in earlier research. The Lewis acidic sites on the nanostructure are believed to enhance the initial Knoevenagel reaction between isatin 3 and malononitrile 2, resulting in the formation of alkene 6 in the presence of Ti_3C_2OH MXene. When 3,4-methylenedioxyphenol 2 is added to alkene 6, it creates the Michael adduct 7, which then cyclizes to form intermediate 8. Compound 4 is generated when intermediate 8 undergoes further tautomerization.

In order to evaluate the benefits of the current method over the previously published procedure, we also evaluated the yields, conditions, scope,

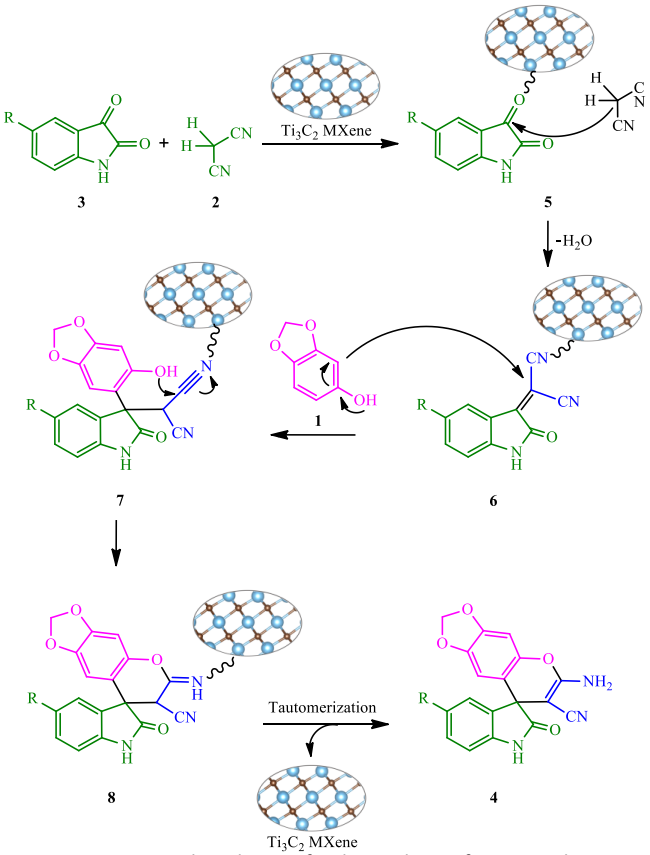

Fig. 7. Proposed mechanism for the synthesis of compound 4.

Table 4. Comparison of the current method with previously published procedure for the preparation of Spiro[3,8′]1,3-dihydro-2*H*-indol-2-one-6′-amino-8′*H*-[1′,3′]dioxolo[4′,5′-*g*][1]benzopyran-7′-yl cyanides.

Conditions	5-Substituted isatins	Yield (%)[a]	Ref.
Isatins (1 mmol), malononitrile (1 mmol), 3,4-methylenedioxyphenol (1 mmol), and TiO_2-CNTs (0.024 g) in H_2O (3 mL), at room temperature, 7-8 h	isatin, 5-Cl-isatin, 5-H_3CO-isatin, 5-H_3C-isatin, 5-O_2N-isatin	91-96	[24]
3,4-Methylenedioxyphenol (1 mmol), malononitrile (1 mmol), 5-substituted isatins (1 mmol), and Ti_3C_2OH MXene (0.05 g), under ethanol-drop grinding, at room temperature, 2o min	isatin, 5-Br-isatin, 5-Cl-isatin, 5-HO-isatin, 5-H_3CO-isatin, 5-H_3C-isatin, 5-O_2N-isatin	90-95	This work

[a]Isolated yield.

and generality of this approach in synthesizing spiro[3,8′]1,3-dihydro-2*H*-indol-2-one-6′-amino-8′*H*-[1′,3′]dioxolo[4′,5′-*g*][1]benzopyran-7′-yl cyanides (Table 4).

CONCLUSION

In this study, we developed a mechanochemical method for synthesizing Ti_3C_2OH MXene and employed it for the first time as an effective heterogeneous catalyst to produce spiro-fused oxindole-dioxolo[*g*][1]benzopyran derivatives. The successful fabrication of the nanocatalyst, which exhibits strong structural integrity, thermal stability, and oxygen-containing surface functionalities, possibly including OH groups, was confirmed through comprehensive characterization tests using FT-IR, XRD, SEM, and EDS. We assessed and validated the target products using melting points, FT-IR spectroscopy, ^{1}H NMR, ^{13}C NMR, and elemental analysis. This approach offers a faster, more efficient, and environmentally friendly alternative compared to traditional methods. From an industrial perspective, this strategy is likely to reduce costs, minimize waste, and enhance energy efficiency.

ACKNOWLEDGMENT

Shahrzad Abdolmohammadi expresses her gratitude to the Research Council of the South Tehran Branch, Islamic Azad University, for their technical help.

CONFLICT OF INTEREST

The authors declare that there is no conflict of interests regarding the publication of this manuscript.

REFERENCES

1. Tandi M, Sharma V, Gopal B, Sundriyal S. Multicomponent reactions (MCRs) yielding medicinally relevant rings: a recent update and chemical space analysis of the scaffolds. RSC Advances. 2025;15(2):1447-1489.
2. Li S, Liu J, Wang ZL, Wei D. Mechano-driven chemical reactions. Green Energy and Environment. 2025;10(5):937-966.
3. Zhou L-M, Qu R-Y, Yang G-F. An overview of spirooxindole as a promising scaffold for novel drug discovery. Expert Opinion on Drug Discovery. 2020;15(5):603-625.
4. Panda SS, Girgis AS, Aziz MN, Bekheit MS. Spirooxindole: A Versatile Biologically Active Heterocyclic Scaffold. Molecules. 2023;28(2):618.
5. Kaur M, Singh B, Singh B, Arjuna A. Synthesis and Evaluation of Novel Spiro[oxindole-isoxazolidine] Derivatives as Potent Antioxidants. J Heterocycl Chem. 2016;54(2):1348-1354.
6. Parthasarathy K, Praveen C, Saranraj K, Balachandran C, Kumar PS. Synthesis, antimicrobial and cytotoxic evaluation of spirooxindole[pyrano-bis-2H-l-benzopyrans]. Med Chem Res. 2016;25(10):2155-2170.
7. Ye N, Chen H, Wold EA, Shi P-Y, Zhou J. Therapeutic Potential of Spirooxindoles as Antiviral Agents. ACS Infectious Diseases. 2016;2(6):382-392.
8. Arun Y, Saranraj K, Balachandran C, Perumal PT. Novel spirooxindole–pyrrolidine compounds: Synthesis, anticancer and molecular docking studies. Eur J Med Chem. 2014;74:50-64.
9. Yu B, Yu D-Q, Liu H-M. Spirooxindoles: Promising scaffolds for anticancer agents. Eur J Med Chem. 2015;97:673-698.
10. Turner H. Spiroindolone Nitd609 is a Novel Antimalarial Drug that Targets the P-type Atpase PfATP4. Future Med Chem. 2016;8(2):227-238.
11. Rojas-Duran R, González-Aspajo G, Ruiz-Martel C, Bourdy G, Doroteo-Ortega VH, Alban-Castillo J, et al. Anti-inflammatory activity of Mitraphylline isolated from Uncaria tomentosa bark. J Ethnopharmacol. 2012;143(3):801-804.
12. Efange NM, Lobe MMM, Keumoe R, Ayong L, Efange SMN. Spirofused tetrahydroisoquinoline-oxindole hybrids as a novel class of fast acting antimalarial agents with multiple modes of action. Sci Rep. 2020;10(1).
13. Bhandari S, Sana S, Lahoti V, Tokala R, Shankaraiah N. Ring-opening cyclization of activated spiro-aziridine oxindoles with heteroarenes: a facile synthetic approach to spiro-oxindole-fused pyrroloindolines. RSC Advances. 2020;10(27):16101-16109.
14. Al-Rashood ST, Hamed AR, Hassan GS, Alkahtani HM, Almehizia AA, Alharbi A, et al. Antitumor properties of certain spirooxindoles towards hepatocellular carcinoma endowed with antioxidant activity. Journal of Enzyme Inhibition and Medicinal Chemistry. 2020;35(1):831-839.
15. Dahlqvist M, Rosen J. The rise of MAX phase alloys – large-scale theoretical screening for the prediction of chemical order and disorder. Nanoscale. 2022;14(30):10958-10971.
16. Sharma VS, Mishra S, Sharma AS, Sharma N, Varma RS, Shrivastav PS, et al. Microcrystalline Cellulose and Cellulose Nanocrystals: Ecofriendly and Sustainable Support Materials in Heterogeneous Nanocatalysis for Green Organic Transformations. Asian Journal of Organic Chemistry. 2025;14(2).
17. Dadashi Firouzjaei M, Karimiziarani M, Moradkhani H, Elliott M, Anasori B. MXenes: The two-dimensional influencers. Materials Today Advances. 2022;13:100202.
18. Kewate OJ, Punniyakoti S. Ti_3AlC_2 MAX phase and Ti_3C_2TX MXene-based composites towards supercapacitor applications: A comprehensive review of synthesis, recent progress, and challenges. Journal of Energy Storage. 2023;72:108501.
19. Gogotsi Y, Huang Q. MXenes: Two-Dimensional Building Blocks for Future Materials and Devices. ACS Nano. 2021;15(4):5775-5780.
20. Fard NE, Fazaeli R, Yousefi M, Abdolmohammadi S. Morphology-Controlled Synthesis of CuO, CuO Rod/MWW Composite for Advanced Oxidation of Indole and Benzothiophene. ChemistrySelect. 2019;4(33):9529-9539.
21. Elmi Fard N, Fazaeli R, Yousefi M, Abdolmohammadi S. Oxidation of carbazole by shape-controllable Cu_2O on MWW catalysis. Appl Phys A. 2019;125(9).
22. Abdolmohammadi S, Hossaini Z, Poor Heravi MR. PANI-Fe_3O_4@ZnO nanocomposite as magnetically recoverable organometallic nanocatalyst promoted synthesis of new Azo chromene dyes and evaluation of their antioxidant and

antimicrobial activities. Mol Divers. 2021;26(4):1983-1993.
23. Janitabar-Darzi S, Abdolmohammadi S. TiO_2–SiO_2 nanocomposite as a highly efficient catalyst for the solvent-free cyclocondensation reaction of isatins, cyclohexanones, and urea. Zeitschrift für Naturforschung B. 2019;74(7-8):559-564.
24. Abdolmohammadi S, Rasouli Nasrabadi SR, Dabiri MR, Banihashemi Jozdani SM. TiO_2 Nanoparticles Immobilized on Carbon Nanotubes: An Efficient Heterogeneous Catalyst in Cyclocondensation Reaction of Isatins with Malononitrile and 4-Hydroxycoumarin or 3,4-Methylenedioxyphenol under Mild Reaction Conditions. Appl Organomet Chem. 2020;34(4).
25. Janitabardarzi S, Shariati M, Sillanpää M. Tailoring MXenes for Effective Water Purification: Recent Advances in Material Properties and Environmental Applications. Korean J Chem Eng. 2026;43(5):1315-1353.
26. Kis VK, Kovács Z, Czigány Z. Improved Method for Electron Powder Diffraction-Based Rietveld Analysis of Nanomaterials. Nanomaterials. 2024;14(5):444.
27. Shahin N, Kazemi S, Heidarpour A. Mechanochemical synthesis mechanism of Ti_3AlC_2 MAX phase from elemental powders of Ti, Al and C. Adv Powder Technol. 2016;27(4):1775-1780.
28. Kim S, Nam S-N, Park CM, Jang M, Taheri-Qazvini N, Yoon Y. Effect of single and multilayered Ti_3C_2TX MXene as a catalyst and adsorbent on enhanced sonodegradation of diclofenac and verapamil. J Hazard Mater. 2022;426:128120.